PNAS RESEARCH ARTICLE | EARTH, ATMOSPHERIC, AND PLANETARY SCIENCES
EVOLUTION

Extremely rapid, yet noncatastrophic, preservation of the flattened-feathered and 3D dinosaurs of the Early Cretaceous of China

Scott A. MacLennan[a,b,1], Jingeng Sha[c,1], Paul E. Olsen[d,1], Sean T. Kinney[d], Clara Chang[d], Yanan Fang[c], Jun Liu[e], Bennett B. Slibeck[d], Elaine Chen[f], and Blair Schoene[b]

Affiliations are included on p. 6.

Contributed by Paul E. Olsen; received February 20, 2024; accepted August 27, 2024; reviewed by Terrence Blackburn, Bhart-Anjan S. Bhullar, and E. T. Rasbury

Northeast China's Early Cretaceous Yixian Formation preserves spectacular fossils that have proved extraordinarily important in testing evolutionary hypotheses involving the origin of birds and the distribution of feathers among nonavian dinosaurs. These fossils occur either flattened with soft tissue preservation (including feathers and color) in laminated lacustrine strata or as three-dimensional (3D) skeletons in "life-like" postures in more massive deposits. The relationships of these deposits to each other, their absolute ages, and the origin of the extraordinary fossil preservation have been vigorously debated for nearly a half century, with the prevailing view being that preservation was linked to violent volcanic eruptions or lahars, similar to processes that preserved human remains at Pompeii. We present high-precision zircon U-Pb geochronology from cores and outcrops, demonstrating that Yixian Formation accumulation rates are more than an order of magnitude higher than usually estimated. Additionally, we provide zircon provenance and sedimentological data from 3D dinosaur fossils, which imply that their death and burial occurred in collapsed burrows, rather than via a catastrophic volcanogenic mechanism. In the studied area, the three principal fossil-rich intervals of the Yixian occur as a cyclic sequence that correspond to periods of high precipitation. Using Bayesian–Markov Chain Monte Carlo approaches, we constrain the total duration of the sequence to less than ~93,000 y and suggest that climatic precession paced the expression of these cyclic sediments. Rather than representing multiple, Pompeii-like catastrophes, the Yixian Formation is instead a brief snapshot of normal life and death in an Early Cretaceous continental community.

Jehol Biota | Early Cretaceous | U-Pb geochronology | lacustrine astrochronology | taphonomy

Significance

Traditionally, the spectacular preservation of fossils of feathered dinosaurs and early birds and other animals found in sedimentary strata of the Yixian Formation in northeast China has been attributed to Pompeii-like volcanic catastrophes. We provide high-resolution geochronology and sedimentological analysis challenging this model and show that these strata instead record normal life and death processes preserved in a succession of depositional environments that span less than 100 thousand years.

The continental, Early Cretaceous age Yixian Formation in Liaoning and Inner Mongolia, China, preserves remarkable fossil assemblages, broadly termed the Jehol Biota, that have revolutionized our understanding of dinosaurian paleobiology and Early Cretaceous ecosystems (1–6). In the areas near the villages of Sihetun, Huangbanjigou, and Lujiatun, these fossil assemblages occur in two famously productive, distinct lithostratigraphic members. Flattened feathered dinosaurs and other organisms with soft tissues are preserved in the lacustrine Jianshangou Member (7, 8), and three-dimensional (3D), perfectly articulated skeletons in life-like postures and associated with apparent nests are found in the Lujiatun Member (8, 9). The mechanism for the seemingly exceptional preservation of these organisms remains contested (e.g., refs. 10 and 11), however, the most commonly favored model (6, 11–14), requires the influence of catastrophic burial in pyroclastics akin to the Vesuvian eruption at Pompeii in AD 79. Indeed, these fossil sites have nicknames that are versions of "China's Cretaceous" Pompeii (6, 11–15). In addition, the temporal and environmental relationships for these assemblages with their divergent taphonomic motifs also remain contentious, impeding a synoptic view of this critical window into Early Cretaceous life.

Major paleobiologically and paleoclimatologically relevant issues regarding the stratigraphic units containing the Jehol biota include: 1) whether the Jianshangou Member with lacustrine flattened fossil assemblages is temporally equivalent to the more terrestrial Lujiatun Member with fossil skeletons preserved in 3D (16, 17), or if these members represent different styles of preservation in successive environments; 2) what time duration the Lujiatun and Jianshangou members record and whether the sedimentological evidence for apparently cyclic environmental fluctuations are orbitally paced at precession (10s of kyr) or eccentricity (100s of kyr) frequencies (11, 18); and 3) whether the Yixian fauna represents catastrophic death assemblages with animals entombed in pyroclastic flows, ashes, or lahars as interpreted by previous studies (6, 11–14) or if more mundane attritional

Author contributions: S.A.M., J.S., S.T.K., P.E.O., and Y.F. designed research; S.A.M., S.T.K., P.E.O., C.C., J.L., B.B.S., E.C., and B.S. performed research; S.A.M., S.T.K., P.E.O., C.C., and B.S. analyzed data; S.A.M. conceptualized project; J.S. and S.T.K. funding; P.E.O. conceptualized project, drafted figures, project administration and supervision, funding; and S.A.M., S.T.K., and P.E.O. wrote the paper.

Reviewers: T.B., University of California, Santa Cruz; B.-A.S.B., Yale University; and E.T.R., Stony Brook University.

The authors declare no competing interest.

[1]To whom correspondence may be addressed. Email: scott.maclennan@wits.ac.za, jgsha@nigpas.ac.cn, or polsen@ldeo.columbia.edu.

This article contains supporting information online at https://www.pnas.org/lookup/suppl/doi:10.1073/pnas.2322875121/-/DCSupplemental.

Published November 4, 2024.

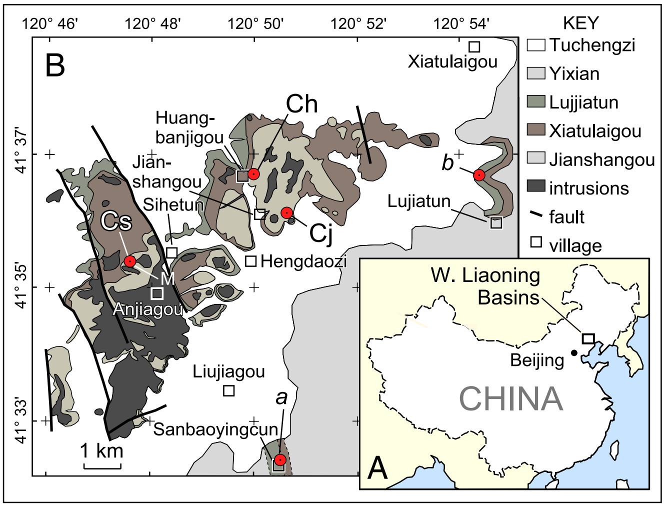

Fig. 1. Location of cores and outcrops. (*A*) Index map showing the location of study area in Liaoning Province, China. (*B*) Geologic map showing key localities (*SI Appendix*, Table S1): *a*, location of Sanbaoyingcun sample; *b*, type section of the Lujiatun Member (8); Ch, Core 1 (Huangbanjiagou no. 1); Cj, Jainshangou no. 1 core; Cs, Core 2 (Sihetun no. 1). Figure adapted from ref. 8 with permission from Elsevier, in which complete core descriptions are found.

models can be applied. Recently published high-resolution $^{40}Ar/^{39}Ar$ and U-Pb geochronological studies have not provided resolution to these problems (16, 19).

To address these issues, we use stratigraphic and sedimentological analysis of drill core and outcrops, U-Pb zircon geochronology via thermal ionization mass spectrometry (TIMS) and a Bayesian statistical approach (20) and laser ablation inductive coupled mass spectrometry (LA-ICP-MS), Huangbanjiagou (8) and Sihetun (Figs. 1 and 2 and *SI Appendix*, Figs. S1–S4), which, critically, contain what we argue are complete sequences of the lower Yixian Formation in unambiguous stratigraphic superposition. Our samples come from within the fossiliferous Lujiatun and Jianshangou Members, including an outcrop exposure of the Lujiatun Member from an area that produced many articulated dinosaurs, as well as matrix from two blocks containing 3D-preserved articulated dinosaurs from this locality. Our integrated geological context allows for the construction of a high-precision age model for the local stratigraphy, permitting tests of hypotheses concerning the contemporaneity of stratigraphic members, orbital pacing of cyclic sediments, and mode of preservation (Figs. 2 and 3).

The prevalent interpretation of lower Yixian Formation stratigraphy (hypothesis 1 in Fig. 2*A*) has the Jianshangou Member deep-water lake sequence laterally equivalent to the outcropping, 3D-dinosaur-producing, supposedly shoreline facies Lujiatun Member outcrops. This hypothesis requires two lava flow sequences, two Lujiatun-like units, and requires that the Xiatulaigou Member flows (Lava 1 in Fig. 2) were not deposited in the Lujiatun area. Here, we present a more parsimonious hypothesis (hypothesis 2 in Fig. 2*A*) that correlates the Lujiatun outcrop with the Lujiatun-like unit in the drillcore and requires only one lava flow sequence (Xiatulaigou Member) and one Lujiatun-like unit. In hypothesis 2, the Jianshangou member is missing due to erosion in the Lujiatun outcrop area.

Critical to testing these hypotheses is drill core Huangbanjiagou No. 1 (Ch in Fig. 1, hereafter termed Core 1), which was drilled directly adjacent to quarries producing typical faunal assemblages of the Jianshangou Member. It spans the complete local stratigraphy of lacustrine finely laminated siliciclastics of the Jianshangou Member with numerous crystal-rich airfall tuffs, the underlying basaltic lavas of the Xiatulaigou Member, and a lower unit characterized by mixed fine and coarse siliciclastics and volcaniclastics that we interpret as representing the Lujiatun Member. These rocks unconformably overlie the Tuchengzi Formation (8) (Figs. 1 and 2 and *SI Appendix*, Fig. S2). The Yixian stratigraphy in this core is very similar to that intersected by another core recovered at the Sihuten geopark, (Sihetun no. 1, Cs in Fig. 1, hereafter Core 2). The basal part of the stratigraphy intersected by core 1 is also similar to outcrops from the Lujiatun Member to the east, where exquisite tetrapod skeletons have been recovered (Fig. 2), but where the overlying Jianshangou Member is not preserved.

Two horizons within core 1 were sampled for U-Pb geochronology. Sample H1-8810 is located at the base of core 1, within siliciclastics in what we hypothesize to be the Lujiatun Member (Fig. 2). This sample is a fluvially reworked volcanoclastic unit based on the presence of stratigraphically proximal polymict conglomerates, and lithic clasts in the sample itself (*SI Appendix*, Fig. S9). A graded airfall tuff (sample H1-3794) associated with the microlaminated lower Jianshangou Member, which overlies the Xiatulaigou Member lavas, was sampled near the middle of the drill core (*SI Appendix*, Figs. S4 and S8). This portion of the drill core bears *Eoestheria* (a clam shrimp) and *Lycoptera* (a teleost fish), typical elements of the Jehol Biota (25). A thin airfall tuff near the local top of the Jianshangou Member (sample 09.22.15-01) was sampled from outcrop adjacent to the drill core and is our highest sample in the local stratigraphy (Fig. 2 and *SI Appendix*, Figs. S3 and S7).

In addition to drill-core-focused-sampling, matrix of two museum specimens of perfectly articulated 3D *Psittacosaurus* (Ceratopsia, Ornithischia) specimens [Institute of Vertebrate Paleontology and Paleoanthropology (Beijing) (IVPP) 18343 and 18344] from the Lujiatun Member outcrops at Sanbaoyingcun, typical of the preservation style of the member, were sampled to determine grain size and detrital zircon provenance (Fig. 3 and *SI Appendix*, Figs. S1, S5, S6, S11, and S12). Samples were collected from both adjacent to the femur and at the edge of the blocks, as far from the skeleton for each specimen as possible. We also collected volcanoclastic mudstone from an outcrop in the same area (sample 09.18.15-05) for geochronological and provenance purposes. The resulting Bayesian–MCMC high-precision age model for the local stratigraphy and provenance and petrological observations on the fossil-bearing volcano-sedimentary rocks permit the testing of the hypotheses outlined above.

Results

We acquired high-precision TIMS U-Pb ages for the three samples from, and adjacent to, core 1 (Fig. 2*B*), as well as for the sample from outcrop at Sanbaoyingcun (*SI Appendix*, section 2b, Fig. S18, and Table S2). The depositional ages of these zircon-bearing volcaniclastic horizons were estimated using a Bayesian-MCMC method (20). These depositional ages were then used to establish a Bayesian, stratigraphic age model for core 1 (Fig. 1). The depositional age estimates for the four samples that span the stratigraphy at Huangbanjigou, and the Bayesian stratigraphic age model derived from them, show that Yixian Formation sediments in the Sihetun-Huangbanjigou area record an extremely short time period of 49 +40/−49 kyrs at this locality (Fig. 2). A distribution of duration estimates for lower Yixian Formation deposition arise from our age model and the 99th percentile of this distribution is ~93 kyr, implying that it is extremely unlikely that deposition of the Yixian Formation in this area lasted for more than 100 kyr. While there are indications of fluvial reworking of the Lujiatun Member in core, outcrop and thin section (*SI Appendix*, Figs. S9–S13), the graded tuff bed in the middle of the Jianshangou

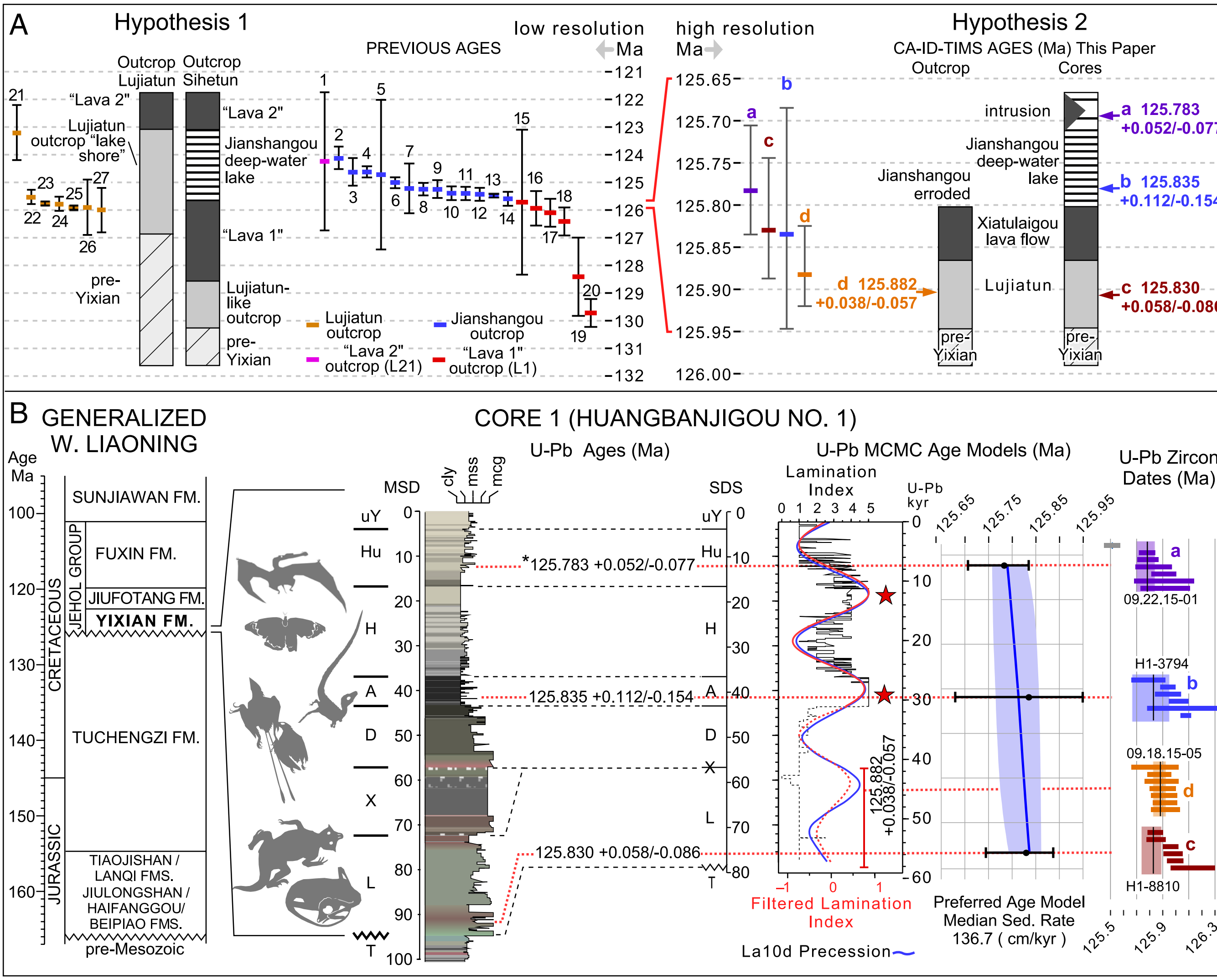

Fig. 2. Temporal constraints and hypotheses for relationships between fossil-bearing units of the Yixian Formation. (*A*) Diagrammatic representation of the two hypotheses for correlation of the Yixian Formation in the Sihetun-Huangbanjiagou area (cores) to Lujiatun area (outcrop) with geochronological constraints. The vertical axis (time) of each hypothesis is shown separately with the axis for Hypothesis 2 (*Right*) being a greatly expanded, high-resolution portion of that for Hypothesis 1 (*Left*). Note that the low-resolution (and inaccurate) previous ages allowed for the "Lava 1" to be largely older than the Lujiatun outcrop, while the core stratigraphy and ages do not. Key to ages 1 to 27 in *SI Appendix*, Table S4. (*B*) CA-ID-TIMS zircon ages (this paper), Bayesian Markov Chain Monte Carlo (MCMC) eruption ages (black circles with black error bars) and stratigraphic age model (dark blue model mean with blue shaded area indicating 95% credible interval) and lithologic section of the Yixian Formation in Core 1 (Huangbanjigou no. 1). Sample designated by * is from outcrop adjacent to core 1 and sample 09.18.15-05 is from a more distant outcrop of the Lujiatun Member at Sanbaoyingcun (Fig. 1). Red stars indicate the stratigraphic positions of the major fossil producing Anjiagou and Hengdaozi beds. Fauna silhouettes based on refs. 3, and 21–24, see *SI Appendix*, pt. 1 for outcrop and core details and are placed to the immediate left of the approximate stratigraphic level that produced them. Lithostratigraphic units: uY, undivided Yixian Formation; Hu, Huangbanjigou Bed, Jianshangou Member; H, Hengdaozi Bed, Jianshangou Member; A, Anjiagou Bed, Jianshangou Member; D, Dajianshanzi Bed, Jianshangou Member; X, Xiatulaigou Member (white stippling indicates vesicles); Lujiatun Member (inferred); T, Tuchenngzi Formation. Other abbreviations: MSD, meters stratigraphic depth; SDS, sedimentary stratigraphic depth with Xiatulaigou Member lavas removed; cly, clay; mss, medium sandstone (included ashes); mcg, medium conglomerate.

Member in the core (H1-3794) is an airfall (*SI Appendix*, Fig. S4 *A* and *B*), thus permitting a direct depositional age determination and precluding the possibility of it being a reworked sample of the underlying Lujiatun Member. Our estimate of temporal duration for deposition of the lower Yixian Formation is two orders of magnitude less than the ca. 2 Myr suggested by cyclostratigraphic analysis of magnetic susceptibility in the correlative sequence at Sihetun (18) (Fig. 1), one order of magnitude less than very recent $^{40}Ar/^{39}Ar$ estimates (19), and about half as long as recent U-Pb geochronology suggests (11).

The Sanbaoyingcun outcrop sample (09.18.15-05), which is 7.9 km from core 1, and produces characteristic Lujiatun Member dinosaurs and other animals, yielded a depositional age of 125.882 +0.038/−0.057 Ma, within the uncertainty of the three samples in superposition from the core. This sample is 5 +5/−2 m directly below exposed lavas indistinguishable from the Xiatulaigou Member in the core, supporting the correlation of the basal interval of core 1 with the Lujiatun Member in outcrop Fig. 1 as shown for hypothesis 2 in Fig. 2*A*.

Zircon U-Pb LA–ICP–MS analysis of zircons from samples of matrix from two articulated specimens (IVPP 18343 and 18344: *SI Appendix*, Fig. S6) from the Sanbaoyingcun locality exhibit very similar age spectra with large peaks at ~124 Ma and ~128 Ma (with uncertainties of ca. 5 Myr), comparable to the chemical abrasion isotope dilution thermal ionization mass spectrometry (CA-ID-TIMS) age of 125.882 +0.038/−0.057 Ma for sample 09.18.15-05 from the same locality (Figs. 1 and 3). The U-Pb age of the Lujiatun matrix provides an older bound for the enclosed fossils and the U-Pb ages from the overlying strata provide the younger bound with both sets of ages lying within each other's

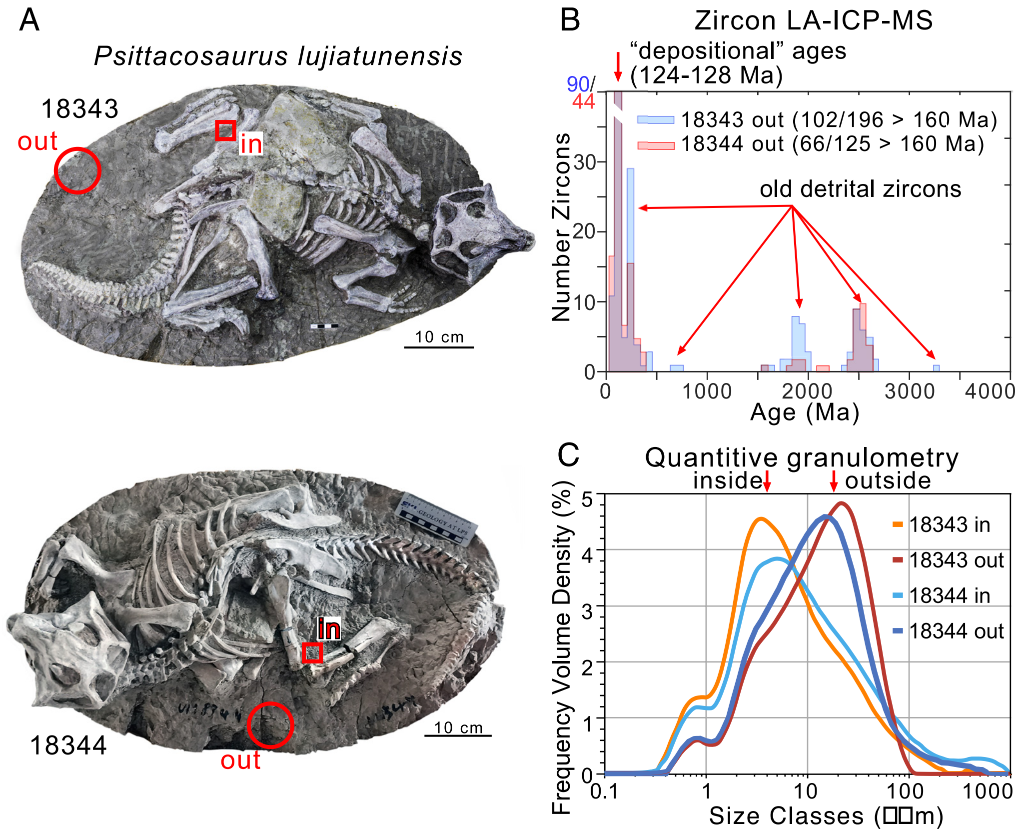

Fig. 3. *Psittacosaurus* Zircon U-Pb laser ablation (LA-ICP-MS) and quantitative diffractive granulometry data from matrix samples for two skeletons specimens of the ornithischian dinosaurs, *Psittacosaurus lujiatunensis*, from the Lujiatun Member at Sanbaoyingcun. (*A*) *P. lujiatunensis* specimens IVPP 18343 (samples P-1, P-2), and IVPP 18344, (samples P-3, P-4) showing the complete and articulated nature of the skeletons in "natural" postures. "in" and "out" refer to samples taken in each specimen, where they are proximal or distal to the skeletons on the position of the samples in being very proximal to the skeleton and out being as distal from the skeleton as possible, interpreted as being inside and outside the burrow, respectively. (*B*) Histogram of zircon dates from matrix distal from to the two dinosaur specimens (out in *B*) showing the age peaks interpreted to result from mixing between a large volcanic depositional age zircon population and detrital zircon sources ranging from the Paleozoic to Precambrian ages, presumably arising from fluvial material from the surrounding drainagearea. (*C*) Quantitative diffusive granulometry data from the two *Psittacosaurus* specimens in A showing the much finer-grained nature of the material proximal to the skeleton (in) versus more distal (out).

uncertainties. The null hypothesis that the two distributions of detrital zircons are the same cannot be rejected ($P = 0.128$), based on results of a Kolmogorov–Smirnov test (26).

Importantly, analysis of these samples reveals a wide range of detrital zircon ages ranging from Mesozoic, through Paleozoic to Archean, revealing contributions from nearby sediment sources during transport and deposition. These detrital zircon age spectra are completely unlike those from airfalls from the Jianshangou Member which lack pre-Mesozoic zircons (11). Thin-section analysis of the fossil matrix samples reveals a tuffaceous polymict sandy siltstone with rounding lithic clasts of varying lithologies (*SI Appendix*, Figs. S10–S12) and even bone clasts (*SI Appendix*, Fig. S13) that are similar to what we argue is the Lujiatun Member in core 1 (*SI Appendix*, Fig. S9). These thin-sections show that the Lujiatun Member in outcrop and core is composed of neither pyroclastic flows nor lahars but are instead simply a reworked, coarse, volcaniclastic mudstone and sandstone.

Laser diffraction particle size analysis (LDPSA) of matrix samples proximal and distal to the 3D *Psittacosaurus* museum skeletal specimens IVPP 18343 and 18344 (Fig. 3 and *SI Appendix*, Fig. S6) reveal a strong and consistent difference in grain size related to proximity to the skeletons in both fossils. Samples external to the skeleton (18343out, 18344out) have a mode between 15 and 21 µm (medium silt). Samples proximal to the skeletons (18343in, 18344in) reveal a fine-grained mode between 3.5 and 5.0 µm (clay to very fine silt).

Discussion

The Dinosaur-Bearing Lujiatun Member Was Not Deposited on a Shoreline of the Jianshangou Lake. Our stratigraphic and geochronological data do not support the hypothesis that the outcropping 3D dinosaur-bearing Lujiatun Member is a lateral equivalent shore deposit to the deep-water Jianshangou Member (Hypothesis 1 in Fig. 1). First, the drill core from Huangbanjigou shows unambiguously that the lacustrine Jianshangou Member overlies the fluvial Lujiatun Member, and therefore, these two facies cannot be time equivalents. Outcrops of the dinosaur-producing Lujiatun Member have lost the stratigraphy above, plausibly due to erosion, resulting in confusion over the true stratigraphic context of these two units until now. This stratigraphic uncertainty necessitated the use of the "upper" lava flow as a lithostratigraphic marker across the two areas. However, the upper lava flow unit in the Sihetun area is actually an intrusive sill as shown by contact relationships and the absence of vesicularity (8) and therefore cannot correlate stratigraphically to the unambiguous lavas above the outcropping Lujiatun Member. Second, our geochronological data from core and outcrop show that the entire Yixian Formation in that area was deposited in less than ~93 kyr, and previous geochronological data (*SI Appendix*, Table S4) suggesting that the Lujiatun and Jianshangou Members were lateral equivalents were too imprecise to test for synchronicity owing to the short period of deposition that we have now demonstrated. Previous studies (reviewed in ref. 27) incorporating a variety of geochronological results from the Yixian Formation have suggested that the Jianshangou Member strata at Sihetun-Huangbanjigou were deposited over a time interval of one or more million years (18, 28). More recent chemical abrasion isotope dilution isotope ratio mass spectrometry (11) and $^{40}Ar/^{39}Ar$ (19) studies estimate shorter intervals of 298 and 665 kyr for the same strata. In contrast, our zircon U-Pb CA-ID-TIMS results show that the total duration recorded across the Yixian Formation at Huangbanjigou is very unlikely to be more than 100 kyr (Fig. 1). Our new results are in agreement with previous high-precision $^{40}Ar/^{39}Ar$ (19, 27) data that show that the ages of the Jianshangou and outcropping Lujiatun Members cannot be distinguished within uncertainty. Combined with evidence of superposition in core, and using Bayesian and MCMC analysis our data places extremely tight constraints on possible correlations between the outcropping Lujiatun Member, with its 3D fauna, and the lacustrine Jianshangou Member, with its flattened fauna and preserved soft tissue. In fact, the stratigraphic superposition exhibited by the Lujiatun and Jianshangou Members in Core 1 is the key observation establishing their true age relationship and supporting our hypothesis 2 (Fig. 2), where the Lujiatun Member is older than the Xiatulaigou lavas, which in turn underlie the Jianshangou Member. Nowhere is there interbedding of Lujiatun and Jianshangou facies.

Cyclicity in the Jianshangou Member is Consistent with Only Two Precession Cycles, Not Eccentricity. Previous work on the Yixian Formation in the same area at this work proposed that these Early Cretaceous lakes fluctuated at eccentricity-scale (100 s of kyr) frequencies. However, we resolve an exceedingly short depositional duration for the Jianshangou Member of less than ~93 kyr, with a corresponding accumulation rate of ~136.7 cm/kyr. This accumulation rate is one to two orders of magnitude higher than the accumulation rate previously estimated for the nearby Sihetun section of 1.70 cm/kyr (18) with a very similar stratigraphy and nearly identical thickness of the highly fossiliferous, feathered-dinosaur-producing Anjiagou Bed of the Jianshangou Member (8). With the new age model for the Huangbanjigou and correlative Sihetun sections, the implications of the finely laminated cyclic sediments at these locations can be reevaluated. Time series analysis of climate proxy data based on sedimentological facies changes [similar to "depth ranks" (29–32)], suggest that the two main fossil bearing units of the Jainshangou Member coincide with perennial chemical stratification which we attribute to greatest lake depth and therefore peak wet intervals (33), namely the Anjiagou and Hengdaozi beds (Fig. 2*B*). Using our cyclostratigraphic model, and informed by the maximum duration permissible via our age model, we demonstrate that the wet intervals are consistent with climate modulation via precession during the Early Cretaceous (Fig. 1 and *SI Appendix*, Fig. S21). Although only two cycles with deeper lake maxima are insufficient to demonstrate they were orbitally paced, the data are completely inconsistent with cyclicity in the eccentricity bands which would require a total duration of the sequence exceeding the most generous interpretation uncertainties of our analysis (49 +40/−49 kyr).

A recent U-Pb study on the Yixian Formation using a slightly different method (chemical abrasion-isotope dilution-isotope ratio mass spectrometry) (11) obtained a significantly younger age for one sample (CY17-17: 125.457 ± 0.051 Ma) for the lower Jianshangou Member (Anjiagou Bed) than both our approximately stratigraphically equivalent H1-3794 sample (125.835 ± 0.112/−0.154 Ma), and our sample 09.22.15-01 that is confidently stratigraphically well above their Jianshangou sample (*SI Appendix*, Fig. S2). Given that we, 1) produce similar ages in both Janshagou samples which are both significantly older than their sample, and 2) that their sample is from less 1.5 m below an igneous sill (Fig. S2A in ref. 11) that may have subtly affected the isotope systematics of those zircons, we regard our ages as more accurate. In addition to ages from the Lujiatun Member that are within uncertainty from ours, they also present results from a sample with a ~1.6 Myr younger age than our youngest sample, but it is from a distant locality, in a different sub-basin, that cannot be placed in relevant stratigraphic context. We regard our ages as more highly resolved and self-consistent indicating a shorter duration for the Yixian formation in the Sihuten area by a factor of about 0.5.

In addition to significant precession-related cyclicity, we also observe higher frequency peaks in the power spectra, that based on our age model, must be sub-Milankovitch in period. This sub-Milankovitch cyclicity (*SI Appendix*, Fig. S5) appears to have a reasonably consistent signal (18, 19) and may represent the kind of millennial-scale climate modulation as has been seen in high-accumulation rate, high-resolution settings elsewhere in the Late Paleozoic (34), Mesozoic (35), and Pleistocene (36), perhaps related to solar pacing. Although our average accumulation rate of 136.7 cm/kyr might appear high, it is in fact comparable to rates seen in many ancient and modern lacustrine deposits such as those of the Early Jurassic formations of the Newark Supergroup of Eastern North America (24 to 200 cm/kyr (32, 37, 38) or Quaternary strata of the African Great lakes and Lake Bosumtwi (10 to 234 cm/kyr) (39–43).

3D Lujiatun Skeletons are Preserved in Collapsed Burrows, Not Intombed by Volcanic Catastrophes. The preservation of 3D skeletons of dinosaurs, dinosaur nests, predation of dinosaurs by mammals (15), and other faunal elements in life-like poses from the outcropping Lujiatun Member has given rise to the idea they were entombed by violent volcanic eruptions, either in hot pyroclastic flows (14) or lahars (44) (volcanic debris flows). However, the Lujiatun animals are not preserved in postures typical of pyroclastic events that killed the victims of Pompeii, with "pugilistic" positions (45) or hyperflexion of the hands and feet (46) but rather are often in positions consistent with sleeping or other normal behavior (21), including predation. The numerous clusters of juveniles in nests, not dispersed, and animals in delicate sleeping positions (47, 48) with an absence of evidence of rolling, crushing, or bone breakage (49) are also completely inconsistent with being entrained in a moving lahar, which are extremely violent. These modes of preservation are instead consistent with death from sudden burrow collapse (50).

We hypothesize that if Lujiatun Member fauna were preserved in burrows, the walls of the collapsed burrows would act as sieves allowing only fine material to filter around the skeletons as the soft parts of the individuals rotted away. This phenomenon would lead to a higher proportion of finer grains in the interior of the skeletons compared to the exterior. Our LDPSA results are consistent with this "burrow sieve" hypothesis showing that matrix exterior to skeletons is three to six times coarser than material proximal to skeletal remains (Fig. 3). These data require the animals to still be fleshed out, not skeletonized, as would happen if they died exposed on the surface and scavenged (for which there is no evidence).

A cylindrical cast, or distinct burrow walls or scratch marks on burrow walls would not be evident in the case of collapsed burrows, because, apart from the entombed inhabitant, there would be little or nothing remaining to separate the sides of the structure. This is the case for collapsed tetrapod burrows of Triassic-Jurassic age (51). Burrow casts are only preserved if the burrow is filled with material, not collapsed. Burrow collapse is still a source of mortality for some extant dinosaurs, such as burrowing birds (52). Some nonavian dinosaurs did burrow, the most convincing examples being dinosaur adults and juveniles in filled, uncollapsed burrows (53), similar in size to the *Psittacosaurus* shown here. A burrow origin is consistent with the abundance of articulated skeletons of multiple juveniles and species in close spatial association within the Lujiatun Formation, including an example of an articulated mammalian carnivore (*Repenomamus*) that preyed on psittacosaurs (15, 54). A plausible interpretation is that the *Psittacosaurus* were primary burrowers and other species either preyed on them or opportunistically inhabited their burrows. A similar phenomena is known to occur with modern aardvarks (55). This interpretation is supported, especially in *P. sinesis* and other Yixian species, by anatomical features such as a relatively stocky body with a robust forelimb with a humerus with large muscle attachment crests, radius, and ulna that are also robust, and short and flattened manual digits, and a relatively short but hyperflexible hind limb. These features have been noted previously as reflecting a semiaquatic habitus (56), but they are at least as consistent, if not more so, with digging behavior. Similar features have been used to infer a burrowing habitus in other dinosaurs as well (57). While it is entirely possible that local catastrophic volcanism played a role in suffocation or seismically triggered entombment, catastrophic action is not required, and essentially random burrow collapse is a parsimonious explanation for the 3D fossil preservation in the Lujiatun Member.

Furthermore, detrital zircon U-Pb LA–ICP–MS spectra from the matrix of the dinosaur skeletons found at the Sanbaoyingcun locality show that while these sediments are rich in volcanic material, they still require provenance from the surrounding areas as indicated by the presence of significant Phanerozoic and Precambrian age peaks. Although it is possible that some lithic grains could be entrained during magmatic ascent from the surrounding crust, which occurred during the eruptions of Vesuvius (58), petrographic examination (*SI Appendix*, Figs. S9–S13) of outcrop material and matrix of the skeletons, along with the detrital zircon age spectra, indicate that it is most simply interpreted as an alluvial or fluvial deposit, pedogenically modified, with a mixture of distantly transported lithic grains, recycled skeletal bits, and proximal reworked volcanic material. Together, with evidence for pedogenic homogenization, recycled bone, and the presence of adjacent conglomerates with well-rounded nonvolcanic clasts make a lahar explanation implausible. Thus, an airfall or pyroclastic flow origin is ruled out and the moniker of a catastrophic "Cretaceous Pompeii" is inappropriate.

Conclusions

The surprising result of our zircon U-Pb geochronology, astrochronology, and sedimentology is that the Jehol Biota of the flattened and 3D fauna of the Jianshangou and Lujiatun members represent in aggregate a very small amount of time (<93 kyr), are in a superpositional sequence, and cannot be lateral equivalents. These sediments cyclically sample similar if not identical ecological assemblages during three successive wet portions of climatic precession cycles, comprising one fossorial biocoenosis (Lujiatun Member) and two thanatocoenoses (Anjiagou and Huangbanjiagou beds of the Jianshangou Member). However, the preservation of the flattened and the 3D fauna are not the result of a Pompeii-like catastrophic series of volcanic processes. Rather, these sediments are millennial-scale geological snapshots in time of diverse continental communities sampled repeatedly by cyclical environmental processes and normal attrition of the communities providing the potential for inferring paleoecology in a higher-resolution way than generally possible.

Materials and Methods

Cores. The cores used in this report were collected in close proximity to important fossil localities in the Sihetun Sub-basin in the western part of the Yixian Basin. Details of the coring and recovered sequences are reported by Wang et al. (8). Samples were taken for geochronological and petrographic analysis with a diamond saw or diamond coring bit. The depth model used by Wang et al. (8) was used to construct the stratigraphic section, but the sample numbers from the core are in original depth determinations as marked on the core boxes.

Outcrop and Specimen Selection. Outcrop samples for geochronology were collected using standard field techniques, with their location recorded via an Apple iPhone. Sample 09.18.15-05 was collected directly adjacent to the drill site in a unit readily identifiable in the core (8). Samples from the *Psittacosaurus* skeletal blocks were provided by J.L. (IVPP). While these blocks were collected by local "farmers," their provenance in this case is clear.

Zircon Geochronology and Age Models. Zircons separation and U-Pb mass spectrometry via TIMS and ICP-MS were conducted using standard techniques as described by Schoene et al. (59) and Arizona LaserChron protocols, respectively. Depositional ages for each dated horizon as well as the resulting stratigraphic age model for Core 1 were calculated using a Bayesian MCMC approach described in refs. 20 and 59. More details around sample description, isotopic data, and analytical methods are available in *SI Appendix*.

Lamination Index. The Yixian lamination index (8) (Fig. 2 and *SI Appendix*, Figs. S2 and S20) is a subjective classification of sedimentary facies amenable to quantitative analysis arranged in a series along an inferred relative water depth gradient from 0 (subaerial exposure, pervasively mud-cracked) to 5 (deep water, microlaminated) similar to depth ranks as described Triassic-Jurassic strata in the eastern North American rift lacustrine sequences (29, 30, 32) but with a lower dynamic range.

Time Series Analysis and Comparison with Astronomical Solutions. Timeseries analysis of the lamination index data was conducted using the Acycle (60) software package, including multitaper spectral estimates (*SI Appendix*, Fig. S20) and TimeOpt accumulation rate estimates (*SI Appendix*, Fig. S22). The astronomical solution used was La10d (61) because it better fits highly resolved, long, early Mesozoic long lacustrine records than other solutions (32). See *SI Appendix* for details.

Granulometry. Samples for quantitative LDPSA were prepared by disaggregation and chemical cleaning followed by being run in water with Mastersizer 3000. See *SI Appendix* for details.

Data, Materials, and Software Availability. All study data are included in the article and/or supporting information.

ACKNOWLEDGMENTS. This work was supported by the Chinese Academy of Geological Sciences and National Committee of Stratigraphy of China (DD20190009) and the National Natural Science Foundation of China (91114201 and 41730317). It is a contribution to UNESCO-IUGS IGCP Project 632 and Project 4 of the CyclcoAstro project. The latter is funded by the Heising-Simons Foundation that provided partial support to P.E.O., S.K., and B.B.S. The Lamont summer intern program is thanked for the support of E.C. The Lamont Climate Center is acknowledged for support to P.E.O., C.C., B.B.S., and S.T.K. We are grateful to three reviewers whose criticisms and suggestions substantially improved the manuscript. We especially thank Bhart-Anjan Bhullar (Yale) for suggestions that anatomical features of *Psittacosaurus* that suggest it was a burrower.

Author affiliations: [a]School of Geosciences, University of the Witwatersrand, Johannesburg 2017, South Africa; [b]Department of Geosciences, Princeton University, Princeton, NJ 08544; [c]State Key Laboratory of Palaeobiology and Stratigraphy, Nanjing Institute of Geology and Palaeontology, Nanjing 210008, China; [d]Biology and Paleo Environment, Lamont-Doherty Earth Observatory of Columbia University, Palisades, NY 10964; [e]Department of Paleoichthyology and Paleoherpetology, Institute of Vertebrate Paleontology and Paleoanthropology, Chinese Academy of Sciences, Beijing 100044, China; and [f]Private address, New York, NY 10019

1. Z. Zhou, P. M. Barrett, J. Hilton, An exceptionally preserved Lower Cretaceous ecosystem. *Nature* **421**, 807–814 (2003).
2. M. Matsukawa, K. Shibata, K. Sato, X. Xing, M. G. Lockley, The early cretaceous terrestrial ecosystems of the Jehol Biota based on food-web and energy-flow models. *Biol. J. Linnean Soc.* **113**, 836–853 (2014).
3. P. J. Chen, Z. M. Dong, S. N. Zhen, An exceptionally well-preserved theropod dinosaur from the Yixian formation of China. *Nature* **391**, 147–152 (1998).
4. F. Mao, C. Zhang, C. Liu, J. Meng, Fossoriality and evolutionary development in two Cretaceous mammaliamorphs. *Nature* **592**, 577 (2021).

5. M. J. Benton, A colourful view of the origin of dinosaur feathers. *Nature* **604**, 630–631 (2022), 10.1038/d41586-022-01036-z.
6. M. J. Benton, Z. Zhonghe, P. J. Orr, Z. Fucheng, S. L. Kearns, The remarkable fossils from the Early Cretaceous Jehol Biota of China and how they have changed our knowledge of Mesozoic life: Presidential Address, delivered 2nd May 2008. *Proc. Geol. Assoc.* **119**, 209–228 (2008).
7. P. Chen *et al.*, Studies on the Late Mesozoic continental formations of western Liaoning. *Bull. Nanjing Inst. Geol. Palaeontol.* **1**, 22–55 (1980).
8. Y. Wang *et al.*, Stratigraphy, correlation, depositional environments, and cyclicity of the Early Cretaceous Yixian and Jurassic-Cretaceous Tuchengzi formations in the Sihetun area (NE China) based on three continuous cores. *Palaeogeogr., Palaeoclimatol., Palaeoecol.* **464**, 110–133 (2016).
9. M. M. Chang, Y. Q. Wang, Y. Wang, *The Jehol Biota* (Scientific and Technical Publishers, Beijing, China, 2003), p. 207.
10. C. S. Rogers *et al.*, The Chinese Pompeii? Death and destruction of dinosaurs in the Early Cretaceous of Lujiatun, NE China. *Palaeogeogr., Palaeoclimatol., Palaeoecol.* **427**, 89–99 (2015).
11. Y. Zhong *et al.*, High-Precision geochronological constraints on the duration of 'Dinosaurs Pompeii' and the Yixian Formation. *Natl. Sci. Rev.* **8**, nwab063 (2021).
12. T. Shao, H. Zhang, Q. Wang, Y. Liu, Y. Zhang, A mesozoic pompeii: History of the Jehol Biota's rise and fall. *Acta Geol. Sin.-Engl. Ed.* **91**, 1893–1903 (2017).
13. M. Zhang, P. Chen, Y. Wang, Y. Wang, *Jehol Biota: Biota: The Emergence of Feathered Dinosaurs, Beaked Birds and Flowering Plants* (Shanghai Scientific and Technical Publishers, Shanghai, China, 2003), p. 208.
14. B. Jiang, G. E. Harlow, K. Wohletz, Z. Zhou, J. Meng, New evidence suggests pyroclastic flows are responsible for the remarkable preservation of the Jehol Biota. *Nat. Commun.* **5**, 1–7 (2014).
15. G. Han *et al.*, An extraordinary fossil captures the struggle for existence during the Mesozoic. *Sci. Rep.* **13**, 11221 (2023).
16. S. Chang, New age constraints on the Yixian formation and its implications for the Jehol Biota. *PaleoBios* **36**, 97 (2019).
17. H. Y. He *et al.*, $^{40}Ar/^{39}Ar$ dating of Lujiatun bed (Jehol Group) in Liaoning, Northeastern China. *Geophys. Res. Lett.* **33**, L04303 (2006).
18. H. Wu *et al.*, Astrochronology for the Early Cretaceous Jehol Biota in northeastern China. *Palaeogeogr., Palaeoclimatol., Palaeoecol.* **385**, 221–228 (2013).
19. Y. Li *et al.*, Rapid preservation of Jehol Biota in Northeast China from high precision $^{40}Ar/^{39}Ar$ geochronology. *Earth Planet. Sci. Lett.* **594**, 117718 (2022).
20. C. B. Keller, B. Schoene, K. M. Samperton, A stochastic sampling approach to zircon eruption age interpretation. *Geochem. Perspect. Lett.* **8**, 31–35 (2018).
21. C. Gao, E. M. Morschhauser, D. J. Varricchio, J. Liu, B. Zhao, A second soundly sleeping dragon: New anatomical details of the Chinese troodontid *Mei* long with implications for phylogeny and taphonomy. *PLoS ONE* **7**, e45203 (2012).
22. J. Lu, A new boreopterid pterodactyloid pterosaur from the Early Cretaceous Yixian Formation of Liaoning Province, Northeastern China. *Acta Geol. Sin. (Engl. Ed.)* **84**, 241–246 (2010).
23. Q. Yang, Y. Zhao, D. Ren, An exceptionally well-preserved fossil Kalligrammatid from the Jehol Biota. *Chin. Sci. Bull.* **54**, 1732–1737 (2009).
24. L. M. Chiappe, M. Qingjin, *Birds of Stone: Chinese Avian Fossils from the Age of Dinosaurs* (Johns Hopkins University Press, Baltimore, MD, 2016).
25. A. W. Grabau, Stratigraphy of China, part 2: Mesozoic. *Bull. Geol. Surv. China* **37**, 1–771 (1928).
26. J. E. Saylor, K. E. Sundell, Quantifying comparison of large detrital geochronology data sets. *Geosphere* **12**, 203–220 (2016).
27. S. Chang, K. Q. Gao, C. F. Zhou, F. Jourdan, New chronostratigraphic constraints on the Yixian formation with implications for the Jehol Biota. *Palaeogeogr., Palaeoclimatol., Palaeoecol.* **487**, 399–406 (2017).
28. H. K. Olierook, F. Jourdan, R. E. Merle, Age of the Barremian–Aptian boundary and onset of the Cretaceous Normal Superchron. *Earth-Sci. Rev.* **197**, 102906 (2019).
29. P. E. Olsen, A 40-million-year lake record of early Mesozoic orbital climatic forcing. *Science* **234**, 842–848 (1986).
30. P. E. Olsen, D. V. Kent, Milankovitch climate forcing in the tropics of Pangea during the Late Triassic. *Palaeogeogr., Palaeoclimatol., Palaeoecol.* **122**, 1–26 (1996).
31. P. E. Olsen, D. V. Kent, Long-period Milankovitch cycles from the Late Triassic and Early Jurassic of eastern North America and their implications for the calibration of the early mesozoic time scale and the long-term behavior of the planets. *Philos. Trans. R. Soc. Lond. A* **357**, 1761–1787 (1999).
32. P. E. Olsen *et al.*, Mapping solar system chaos with the geological orrery. *Proc. Natl. Acad. Sci. U.S.A.* **116**, 10664–10673 (2019).
33. P. E. Olsen, "Tectonic, climatic, and biotic modulation of lacustrine ecosystems: Examples from the Newark Supergroup of eastern North America" in *Lacustrine Basin Exploration: Case Studies and Modern Analogs*, B. Katz, Ed. (1990), pp. 209–224.
34. R. Y. Anderson, Enhanced climate variability in the tropics: A 200 000 yr annual record of monsoon variability from Pangea's equator. *Clim. Past* **7**, 757–770 (2011).
35. D. V. Kent, G. Muttoni, P. Brack, Magnetostratigraphic confirmation of a much faster tempo for sea-level change for the Middle Triassic Latemar platform carbonates. *Earth Planet. Sci. Lett.* **228**, 369–377 (2004).
36. G. Bond *et al.*, A pervasive millennial-scale cycle in North Atlantic Holocene and glacial climates. *Science* **278**, 1257–1266 (1997).
37. P. E. Olsen, R. W. Schlische, M. S. Fedosh, "580 ky duration of the Early Jurassic flood basalt event in eastern North America estimated using Milankovitch cyclostratigraphy" in *The Continental Jurassic*, M. Morales, Ed. (New Mexico Museum of Natural History and Science, Albuquerque, NM, 1996), pp. 11–22.
38. D. V. Kent, P. E. Olsen, Early Jurassic magnetostratigraphy and paleolatitudes from the Hartford continental rift basin (eastern North America): Testing for polarity bias and abrupt polar wander in association with the central Atlantic magmatic province. *J. Geophys. Res.* **113**, B06105 (2008).
39. A. S. Cohen *et al.*, Ecological consequences of early Late Pleistocene megadroughts in tropical Africa. *Proc. Natl. Acad. Sci. U.S.A.* **104**, 16422–16427 (2007).
40. S. Lund, E. Platzman, C. Scholz, Late-Holocene paleomagnetic secular variation records from Lake Turkana, East Equatorial Africa. *Holocene* **32**, 321–333 (2022).
41. A. P. Burnett, M. J. Soreghan, C. A. Scholz, E. T. Brown, Tropical East African climate change and its relation to global climate: A record from Lake Tanganyika, Tropical East Africa, over the past 90+ kyr *Palaeogeogr., Palaeoclimatol., Palaeoecol.* **303**, 155–167 (2011).
42. R. L. Lupien *et al.*, A leaf wax biomarker record of early Pleistocene hydroclimate from West Turkana, Kenya. *Q. Sci. Rev.* **186**, 225–235 (2018).
43. T. M. Shanahan *et al.*, The formation of biogeochemical laminations in Lake Bosumtwi, Ghana, and their usefulness as indicators of past environmental changes. *J. Paleolimnol.* **40**, 339–355 (2008).
44. Q. Zhao, P. M. Barrett, D. A. Eberth, Social behaviour and mass mortality in the basal ceratopsian dinosaur *Psittacosaurus* (Early Cretaceous, People's Republic of China). *Palaeontology* **50**, 1023–1029 (2007).
45. P. Petrone, The Herculaneum victims of the 79 AD Vesuvius eruption: A review. *J. Anthropol. Sci.* **97**, 1–22 (2019).
46. G. Mastrolorenzo *et al.*, Herculaneum victims of Vesuvius in AD 79. *Nature* **410**, 769–770 (2001).
47. Q. Zhao, M. J. Benton, X. Xu, P. M. Sander, Juvenile-only clusters and behaviour of the Early Cretaceous dinosaur *Psittacosaurus*. *Acta Palaeontol. Pol.* **59**, 827–833 (2014).
48. Q. Meng, J. Liu, D. J. Varricchio, T. Huang, C. Gao, Parental care in an ornithischian dinosaur. *Nature* **431**, 145–146 (2004).
49. P. J. Baxter, Medical effects of volcanic eruptions. *Bull. Volcanol.* **52**, 532–544 (1990).
50. Y. Yang, W. Wu, P. E. Dieudonné, P. Godefroit, A new basal ornithopod dinosaur from the Lower Cretaceous of China. *PeerJ* **8**, e9832 (2020).
51. H.-D. Sues, P. E. Olsen, Stratigraphic and temporal context and faunal diversity of Permian-Jurassic continental tetrapod assemblages from the Fundy rift basin, eastern Canada. *Atl. Geol.* **51**, 139–205 (2015).
52. P. J. Seddon, Y. van Heezik, Effects of hatching order, sibling asymmetries, and nest site on survival analysis of Jackass Penguin chicks. *Auk* **108**, 548–555 (1991).
53. D. J. Varricchio, A. J. Martin, Y. Katsura, First trace and body fossil evidence of a burrowing, denning dinosaur. *Proc. R. Soc. B* **274**, 1361–1368 (2007).
54. Y. Hu, J. Meng, Y. Wang, C. Li, Large Mesozoic mammals fed on young dinosaurs. *Nature* **433**, 149–152 (2005).
55. U. Rahm, "Tubulidentates: Aardvark" in *Grzimek's Encyclopedia of Mammals. 4*, S. P. Parker, Ed. (McGraw-Hill Publishing Company, New York, NY, 1990), pp. 450–458.
56. T. L. Ford, L. D. Martin, "A semi-aquatic life habit for *Psittacosaurus*" in *New Perspectives on Horned Dinosaurs: The Royal Tyrrell Museum Ceratopsian Symposium*, M. J. Ryan, B. J. Chinnery-Allgeier, D. A. Eberth, Eds. (Indiana University Press, Bloomington, IN, 2010), pp. 328–339.
57. H. M. Avrahami, P. J. Makovicky, R. T. Tucker, L. E. Zanno, A new semi-fossorial thescelosaurine dinosaur from the Cenomanian-age Mussentuchit Member of the Cedar Mountain Formation, Utah. *Anat. Rec.*, 10.1002/ar.25505 (2024).
58. R. Cioni, R. Santacroce, A. Sbrana, Pyroclastic deposits as a guide for reconstructing the multi-stage evolution of the Somma-Vesuvius Caldera. *Bull. Volcanol.* **61**, 207–222 (1999).
59. B. Schoene *et al.*, U-Pb constraints on pulsed eruption of the Deccan Traps across the end-Cretaceous mass extinction. *Science* **363**, 862–866 (2019).
60. M. Li, L. Hinnov, L. Kump, Acycle: Time-series analysis software for paleoclimate research and education. *Comput. Geosci.* **127**, 12–22 (2019).
61. J. Laskar, A. Fienga, M. Gastineau, H. Manche, La2010: A new orbital solution for the long-term motion of the Earth. *Astron. Astrophys.* **532**, 1–15 (2011).